

Direct measurement of the supernova rate in starburst galaxies

J.D. Bregman¹, P. Temi¹, and D. Rank²

¹ NASA Ames Research Center, Moffett Field, CA 94035, USA (jbregman@mail.arc.nasa.gov; temi@ssa1.arc.nasa.gov)

² University of California Santa Cruz, Santa Cruz, CA 95064, USA (rank@ucolick.org)

Received 8 November 1999 / Accepted 21 December 1999

Abstract. Supernovae play a key role in the dynamics, structure, and chemical evolution of galaxies. The massive stars that end their lives as supernovae live for short enough times that many are still associated with dusty star formation regions when they explode, making them difficult to observe at visible wavelengths. In active star forming regions (galactic nuclei and starburst regions), dust extinction is especially severe. Thus, determining the supernova rate in active star forming regions of galaxies, where the supernova rate can be one or two orders of magnitude higher than the average, has proven to be difficult. From observations of SN1987A, we know that the [NiII] 6.63 μm emission line was the strongest line in the infrared spectrum for a period of a year and a half after the explosion. Since dust extinction is much less at 6.63 μm than at visible wavelengths ($A_{6.63}/A_V = 0.025$), the [NiII] line can be used as a sensitive probe for the detection of recent supernovae. We have observed a sample of starburst galaxies at 6.63 μm using ISOCAM to search for the [NiII] emission line characteristic of recent supernovae. We did not detect any [NiII] line emission brighter than a 5σ limit of 5 mJy. We can set upper limits to the supernova rate in our sample, scaled to the rate in M82, of less than 0.3 per year at the 90% confidence level using Bayesian methods. Assuming that a supernova would have a [NiII] line with the same luminosity as observed in SN1987A, we find less than 0.09 and 0.15 per year at the 50% and 67% confidence levels. These rates are somewhat less if a more normal type II supernova has a [NiII] line luminosity greater than the line in SN1987A.

Key words: stars: supernovae: general – galaxies: starburst

1. Introduction

While the supernova rate is one of the key parameters in models of starburst galaxies, constraining the initial mass function and rate of star formation, its value is difficult to measure (Doane & Mathews 1993). Observational approaches have been used to determine this rate, including observations of compact radio sources (Kronberg et al. 1985; Antonucci & Ulvestad 1988; Van Buren & Greenhouse 1994) and direct visible light imaging (Richmond et al. 1998). The

radio observations suffer from confusion since there are a large number of point sources, and there is an uncertainty in the ages of the supernova remnants, leading to a range in the calculated supernova rate of 0.08–0.3 supernovae per year in M82. The optical observations did not detect any supernovae within the starburst regions of the observed galaxies, leading the authors to conclude that there was too much obscuration within the galaxies' nuclei to allow supernovae to be observed at visible wavelengths.

Van Buren & Norman (1989) suggested that supernovae in starburst galaxies could be directly observed in the infrared by imaging the galaxies in the [CoII] 10.52 μm emission line (from radioactive cobalt) since it would be a unique signature of a supernova and would provide information about the mass of the supernova. However, this line is almost coincident with the 10.51 μm [SIV] emission line that is prevalent in planetary nebulae and HII regions. The [CoII] line, from ⁵⁶Co, does decay with a half life of 77 days, so it would be possible to distinguish the difference between [SIV] and [CoII] lines by their temporal behavior if the [CoII] line was spatially separated from [SIV] line emission and it was a substantial fraction of the energy at 10.52 μm . Infrared spectra of SN1987A taken from the Kuiper Airborne Observatory (Rank et al. 1988; Wooden et al. 1993) showed the [CoII] line in emission, but a [NiII] emission line, from ⁵⁸Ni, at 6.63 μm was stronger and persisted longer than any other mid-IR line. The emission lines appear after the peak of the visible light curve when the envelope becomes optically thin, about 120 days after the explosion. The [NiII] line was not evident in a spectrum obtained 60 days after the explosion, but was already a strong line at the next time of observation 260 days after the explosion. The line was weak but still visible at the last observation 775 days after the explosion. Thus, the [NiII] line should be visible in a supernova for nearly 2 years. This line is not seen in any other type of source, it is well separated from any other emission line, and is a unique and long lived supernova indicator which should be relatively free of obscuration from dust within the starburst nucleus.

With the launch of the Infrared Space Observatory (ISO), we were provided the opportunity to search nearby starburst galaxies for recent supernovae by imaging the galaxies at 6.63 μm and at several comparison continuum wavelengths. We did not detect any supernovae in the starburst nuclei, and to this date,

Table 1. Log of ISO Observations

Name	Obs. Date		Int. Time (sec.)	Number of frames
IC 342	10/02/97	-	5.04	233
NGC 253	06/07/97	-	5.04	155
M 82	03/11/97	-	5.04	155
NGC 4449	07/07/96	-	10.08	76
NGC 4945	08/11/96	08/11/97	10.08	229
NGC 5128	08/11/97	-	5.04	155
NGC 5236	07/31/96	08/24/97	10.08	239
CIRCINUS	08/19/96	03/18/97	10.08	232
NGC 6946	10/20/96	04/30/97	10.08	228
NGC 5055	07/13/96	-	10.08	213

no supernova has been detected in a starburst nucleus. In this paper we derive a limit to the supernova rate in starburst nuclei from observations of a sample of galaxies. The observations and data reduction procedure are discussed in Sect. 2, followed by a derivation of the supernova rate in Sect. 3. Our results are summarized in Sect. 4.

2. Observations and data analysis

Images of the galaxies listed in Table 1 were obtained with the infrared camera (ISOCAM) aboard ISO. We were fortunate enough to get two epochs of observations for some of the galaxies, extending the coverage time by about a year for those we observed twice. Since we did not initially know the best way to observe using ISOCAM, the first set of observations were made in a non-optimum manner using just a single set of continuously variable filter (CVF) settings with spectral resolution of $\lambda/\Delta\lambda \simeq 45$. In the second set of observations, we scanned the CVF from short to long wavelengths, moved the telescope 1.5 pixels, then scanned the CVF in the reverse direction. This provided us with redundant data, allowing us to remove artifacts from internal reflections in the camera. We also found that the longest integration time (20 seconds) produced images with so many cosmic ray trails that it was nearly impossible to remove false signals. The same 10 CVF settings were used for all of the observations, and cover the wavelength range from $6.04\mu\text{m}$ to $7.795\mu\text{m}$, including lines from [NiII] ($6.63\mu\text{m}$), [ArII] ($6.98\mu\text{m}$) and [P α] ($7.45\mu\text{m}$) and adjacent continuum. For all of the observations we used the CAM04 AOT with 3 arcsec per pixel. A log of the observations is given in Table 1.

2.1. Data reduction

Data reduction has been performed using the Camera Interactive Analysis (CIA) package. The new release uses the latest calibration files available and some new algorithms for detector characterization and behavior. For the dark current subtraction, a *dark model* has been used to take into account the long term-drift in the dark current which occurred during the ISO mission. Great effort has been devoted to removing cosmic ray hits on

the detector. In order to make a detection of a supernova event, we produced continuum subtracted images of our target galaxies at $6.63\mu\text{m}$. The galaxy's nucleus itself is a fairly bright point-like source, but the expected supernova signature is of the order of a few to tens of mJy. Thus, a clear detection on the subtracted frames relies heavily on the removal of cosmic rays and correction for the glitch-induced transient responses. Most of the short term duration glitches can be easily removed using a sigma clipping filter or multi-resolution method. These glitches are produced by protons and electrons hitting the detector and their effects on the data are the typical spikes present on a pixel time history plot. The spike duration is shorter than the integration time and they last for no more than one or two readouts. Highly energetic protons and electrons and heavy ions are responsible for glitches that cannot be easily removed. For these *special* glitches that introduce a gain variation with a very long time constant in which the stabilization can be very slow, there is no method at the present time that corrects the effect in a satisfactory way. However, since we had redundancy in our data, we were able to check for remnants of long term response variations and either remove or mask these occurrences on the original CVF scan data frames.

The standard calibration file *cal-g* that comes along with the data products is not very well suited for flat field correction with data taken with the CAM04 AOT. We built our own flat field combining calibration files that match our specific data set. After dark current correction, deglitching and stabilization, we can represent a set of data taken with the camera in the same configuration *c*, imaging a source on the array, as

$$I_{\text{obs}}(x, y, c) = \{F_{\text{Source}}(x, y) + F_{\text{Zod}}(x, y)\} \times dflat(x, y) \times oflat(x, y) + F_{\text{Sca}}(x, y) \times dflat(x, y) \quad (1)$$

The library flat field is separated in two distinct frames: the optical flat and the detector flat. Here, $F_{\text{Zod}}(x, y)$, $oflat(x, y)$ and $dflat(x, y)$ correspond to the Zodiacal light, the optical flat and the detector flat respectively as a function of pixel position (x, y) . $F_{\text{Sca}}(x, y)$ is the scattered light pattern which is produced inside the camera between detector and filter and is thus unaffected by the $oflat(x, y)$. We can re-write the same relation as

$$I_{\text{obs}}(x, y, c) = F_{\text{Source}}(x, y) \times oflat(x, y) \times dflat(x, y) + \{F_{\text{Zod}}(x, y) \times oflat(x, y) + F_{\text{Sca}}(x, y)\} \times dflat(x, y) \quad (2)$$

If the source does not produce too much scattered light, $F_{\text{Sca}}(x, y)$ can be ignored and the second term in Eq. (2) can be measured by scanning the zodiacal light. A good quality data cube for the zodiacal light, covering the entire CVF wavelength range, is not available yet. Using library CVF flat images, we built, by interpolation, a datacube that matches the wavelengths in our measurements. Scaling this cube to the intensity measured off-source in our observations, and subtracting

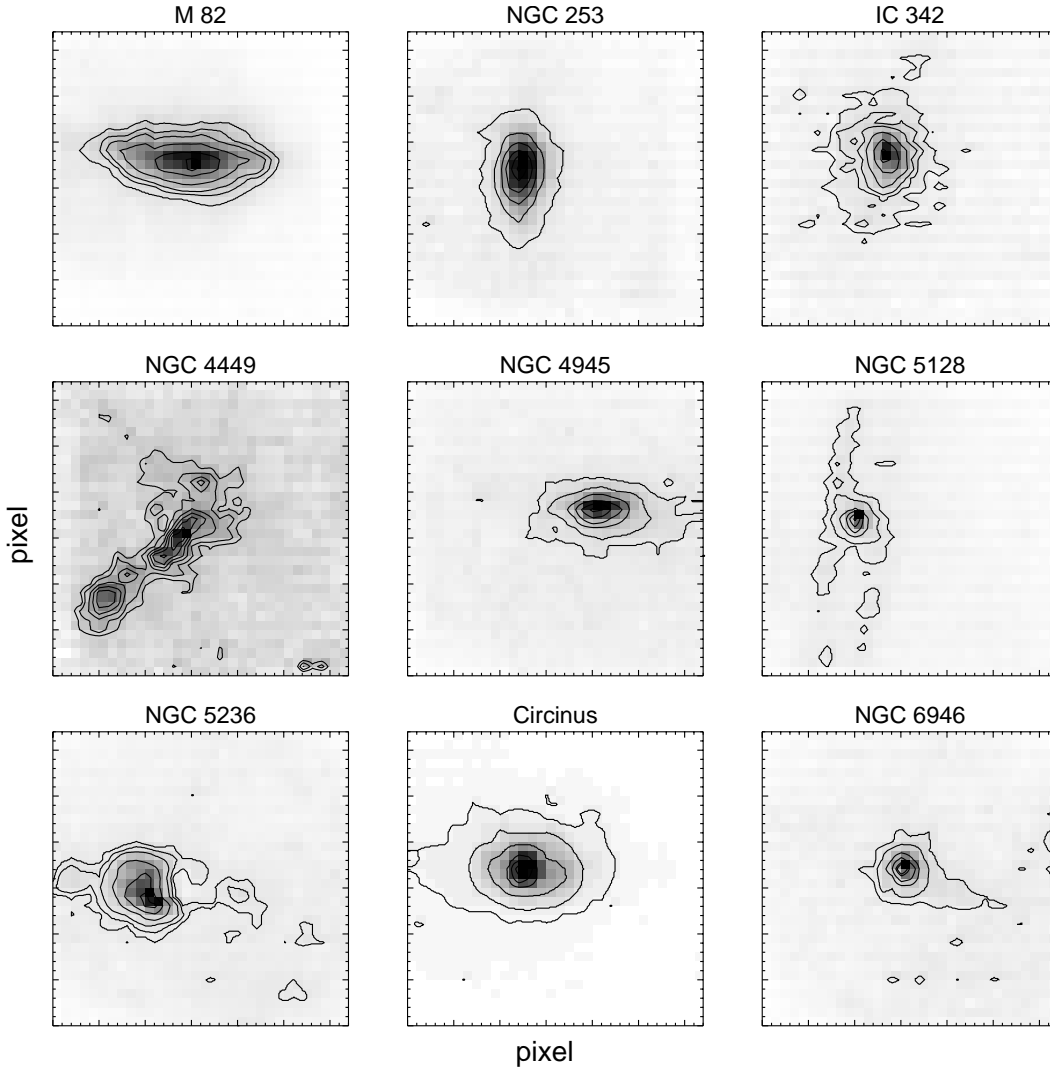


Fig. 1. Gray scale images of the galaxy sample at $6.63 \mu\text{m}$ overlaid with contour lines. Gray scale images are shown with the original 3 arcsec/pixel scale, while the contours have been smoothed with a 3 pixel FWHM gaussian filter. The lower contour in each galaxy is down to a level equal to a noise of 5σ .

the scaled cube from the original data set, we are left with the $F_{\text{Source}}(x, y) \times oflat(x, y) \times dflat(x, y)$ term. The optical flat shows little structure in the central part of the array where our sources are centered. Thus there is no need to correct for it. This is not the case for the detector flat. We recovered some detector flats from the narrow band filter calibration files, and re-sampled them to match the wavelengths in our CVF scan. This way we created a detector flat cube we could use to flat field our data.

Fig. 1 shows a panel of our galaxy sample. For each set of CVF scans we have produced $6.63 \mu\text{m}$ continuum subtracted images; the 1σ rms noise level on these maps is of the order of 0.8 mJy per pixel. Fig. 2 displays a subtracted frame for IC 342 as an example of a fully reduced image. Low frequency noise from glitches is the major contributor to the overall noise. If a possible detection was present in one frame, we had the opportunity to confirm the detection using the data taken with the CVF scanned in the opposite direction. We did not detect any clear emission from a supernova explosion in our sample.

3. Discussion

3.1. Comparison of [NiII] luminosity in SN1987A to a normal supernova

Since the progenitor of SN1987A was a blue supergiant rather than a red supergiant, its peak visual magnitude was about 2 magnitudes less than an average Type II supernova. But SN1987A is also the only supernova bright enough to have been observed in the mid-infrared, and our knowledge of the [NiII] luminosity in supernovae is based solely on this one object. We therefore need to know how SN1987A compares to other Type II supernovae before we can determine the expected brightness of a supernova produced [NiII] line in other galaxies.

The radioactive tail of a supernova light curve is produced by thermalization of gamma rays from ^{56}Co decay. The ^{56}Co itself comes from rapid decay of the ^{56}Ni produced in the supernova explosion. In most supernovae, a predictable fraction of the gamma rays are absorbed in the expanding envelope,

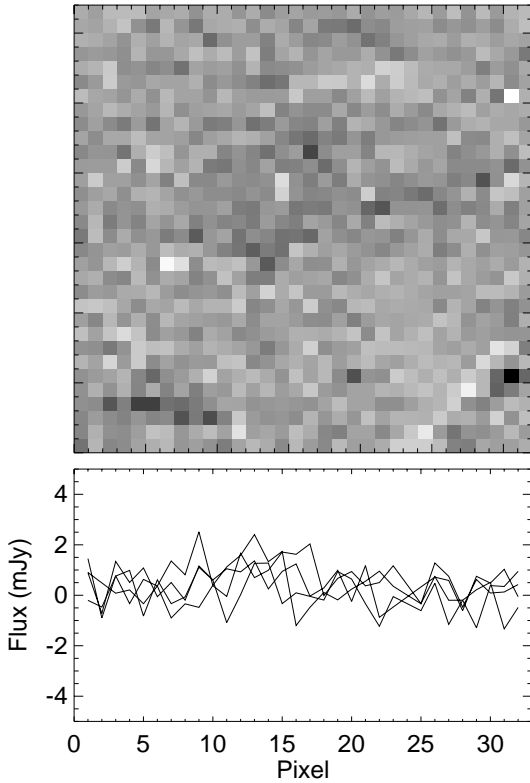


Fig. 2. $6.63 \mu\text{m}$ continuum subtracted image of IC 342. Three row plots taken in the central region of the image show the peak to peak noise of the order of 3 mJy. A residual cosmic ray strip is seen in the lower right corner of the image.

so that the luminosity on the tail is a good indication of the amount of ^{56}Ni produced by the supernova.

Most of the heterogeneity of the light curves in type II supernovae is confined to within 100 days of the explosion. The shape of the curves at later phases seems to converge, except for very few peculiar SNs, to a common behaviour leading to the conclusion that many type II supernovae produce almost the same amount of ^{56}Ni (Patat et al. 1994; Turatto et al. 1998) as expected from a theoretical calculations of ^{56}Ni production (see Fig. 3). Even though SN1987A did not achieve the peak luminosity of most Type II supernovae, due to its compact progenitor, it did have about the same luminosity as typical Type IIs after its peak and therefore had produced about the same amount of ^{56}Ni as a typical Type II supernova.

The [NiII] $6.63 \mu\text{m}$ line observed in SN1987A is a collisionally excited ground state forbidden line of ^{58}Ni , which is also produced in the supernova explosion, and, like the bolometric luminosity, follows the energy deposited by radioactive decay of ^{56}Co . Gamma rays from the cobalt ionize the gas in the supernova envelope, heating the electrons. The [NiII] line intensity therefore depends on the density, on the quantity of ^{56}Ni and ^{58}Ni produced in the explosion, on the fraction of Ni and Ni^+ , and on the temperature of the gas. Note that there were no doubly ionized species observed in SN1987A (Wooden et al. 1993). The [NiII] line becomes visible when the optical depth in the

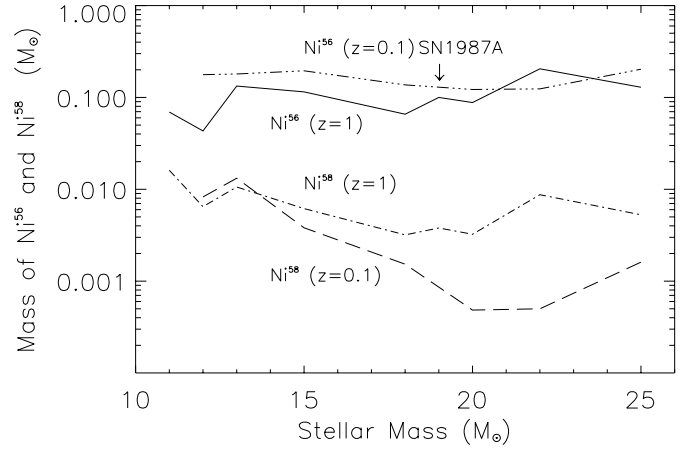


Fig. 3. The masses of ^{56}Ni and ^{58}Ni produced in a supernova explosion as calculated by Woosley & Weaver (1995) are shown as a function of stellar mass for both solar and 0.1 solar metallicity. ^{56}Ni rapidly decays to ^{56}Co which then produces the gamma rays that power the supernova during the tail phase when forbidden lines are visible. ^{58}Ni is stable and is the source of the [NiII] $6.63 \mu\text{m}$ emission line.

expanding envelope becomes optically thin above the NiII zone, and is roughly coincident with the start of the tail phase of a supernova. A typical Type II supernova takes 40-60 days to reach this phase, while the much slower expanding SN1987A took 120 days. However, the combined slower expansion (Woosley 1988) and longer time results in the density of the NiII zone being about the same in SN1987A as in a typical type II. Also, due the high density of the NiII emitting region, the [NiII] $6.63 \mu\text{m}$ line intensity is only linearly dependent on the density. The amount of radioactive ^{56}Ni and stable ^{58}Ni produced as a function of mass and metallicity have been calculated by Woosley & Weaver (1995), and are plotted in Fig. 3 for both solar and 0.1 solar metallicity. The LMC is about one third solar, so we would expect the Ni production to lie between these two curves. For comparison, $0.075 M_{\odot}$ of ^{56}Ni was produced by SN1987A, which agrees quite well with Woosley & Weaver calculations. A good indicator of the trend of the [NiII] emission line intensity is the product of ^{56}Ni and ^{58}Ni , which is shown in Fig. 4. A supernova like SN1987A is near the minimum of the [NiII] line emission as a function of mass, and significantly below that expected for a solar metallicity precursor. Thus, it is likely that the supernovae in galaxies with solar metallicities could have [NiII] emission lines from several times to an order of magnitude as luminous as observed in SN1987A. In our [NiII] emission line estimates, we will use both the SN1987A value ($6 \times 10^{-17} \text{ W cm}^{-2}$ (Wooden et al. 1993) at ≈ 400 days and a value 3 times greater than that observed in SN1987A. However, we should keep in mind that this value is very uncertain, that there is no evidence for $3\times$ greater Ni production in supernovae, and we would learn a lot about [NiII] forbidden line emission if we observe just one supernova.

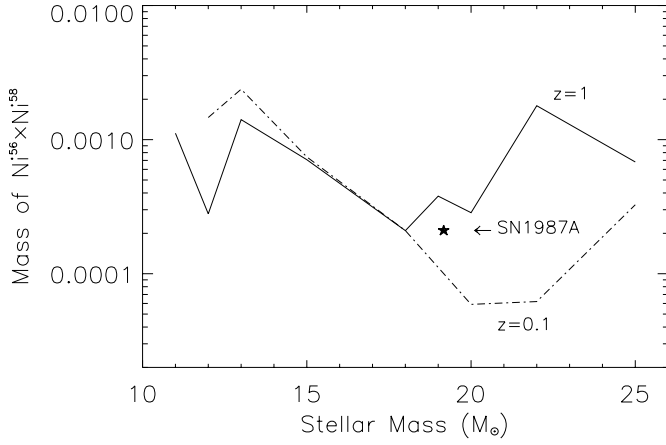


Fig. 4. The product of ^{56}Ni and ^{58}Ni is shown as function of stellar mass of a supernova progenitor for solar and 0.1 solar metallicity stars. Since ^{56}Ni provides the gamma rays to power the supernova and the $6.63\ \mu\text{m}$ line is from ^{58}Ni , their product is an indicator of how the [NiIII] $6.63\ \mu\text{m}$ line should vary with stellar mass and metallicity. The average solar metallicity supernova has a $^{56}\text{Ni} \times ^{58}\text{Ni}$ product 3-4 times that of SN1987A.

3.2. Look time for the sample

The measured [NiIII] line intensity in SN1987A at four different epochs after the explosion (260, 415, 615 and 775 days) are reported by Wooden et al. (1993). The line intensity reaches its peak at 415 days after core collapse with an intensity of $6.15 \times 10^{-17}\ \text{W cm}^{-2}$. At 775 days after collapse, the line intensity drops to $4.37 \times 10^{-18}\ \text{W cm}^{-2}$, but is still the brightest emission line at infrared wavelengths. From these measurements we calculated the expected luminosity of a supernova occurring in each galaxy of the sample. The estimated peak signal that a supernova as bright as SN1987A would produce (in each sample galaxy), is shown in Fig. 5. Since the noise level in the continuum subtracted maps is of the order of 0.8 mJy, we define a visibility time, t^{vis} , as the period of time in which the signal produced at $6.63\ \mu\text{m}$ by the [NiIII] line would be $\geq 5\ \text{mJy}$, in each galaxy in our sample. This will allow us, in case of an event, to make a clear detection with a S/N ratio ≥ 5 .

The visibility time in the sample ranges from $\simeq 1$ year to more than 1.5 years for the closest galaxies; for a supernova with a [NiIII] line emission 3 times brighter than SN1987A the visibility time for the sample increases by about 20%. For NGC 5055 the estimated signal from the [NiIII] line, assuming a supernova as bright as SN1987A, never reaches the 5 mJy level required for a clear supernova detection with our data, while it has a visibility time of 1.2 years assuming a 3 times brighter supernova.

To take into account the fact that some of the galaxies have been observed twice during the ISO mission we need to compute the control time, C^{time} , reference for each galaxy of the sample defined as:

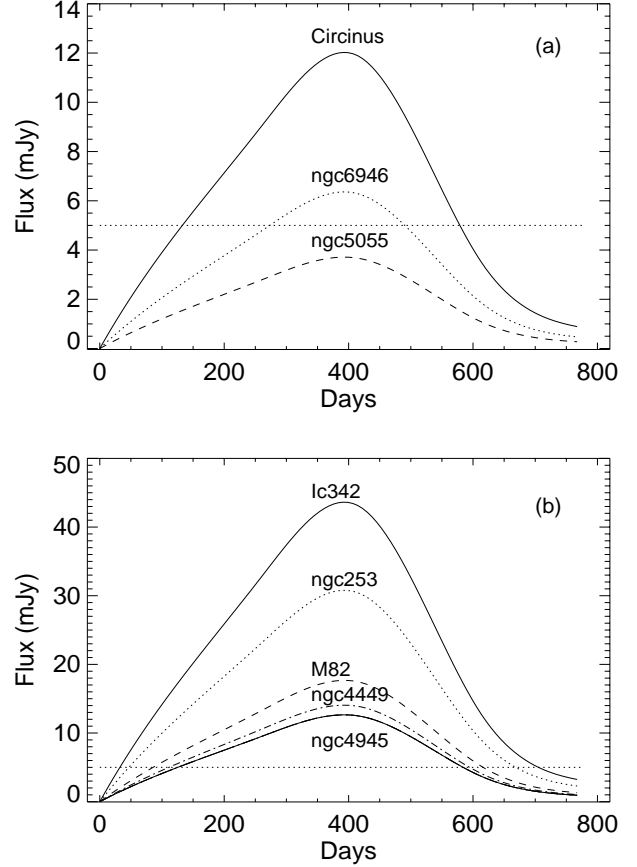


Fig. 5. Visibility time for the galaxy sample. The $5\ \sigma$ limit for a supernova detection is shown as a dotted line. The expected [NiIII] emission line intensities as a function of time after the explosion have been scaled from the measured intensity of SN1987A at different epochs. NGC 5128 and NGC 5236 are not reported in the plot since they have the same distance as NGC 4945.

$$C_j^{\text{time}} = \sum_{i=1}^2 \Delta t_i \quad (3)$$

where:

$$\Delta t_i = \begin{cases} t_i^{\text{vis}} & \text{if } t_i - t_{i-1} \geq t_i^{\text{vis}} \text{ or } i = 1 \\ t_i - t_{i-1} & \text{if } t_i - t_{i-1} \leq t_i^{\text{vis}} \text{ and } i \neq 1 \end{cases} \quad (4)$$

Here t_i is the epoch of the i^{th} observation of the j^{th} galaxy. For those galaxies that have been observed only once, the control time C^{time} coincides with the visibility time t^{vis} . Control times are reported in Column 5 of Table 2.

3.3. Derivation of the rate

In order to derive the supernova rate for the galaxy sample, we need some way of scaling the rates for the individual galaxies.

Table 2. Control Times

Name	d ^a (Mpc)	L _{FIR} (10 ¹⁰ L _⊙)	SN Peak (mJy)	Control Time (Days)	Control Time(3x) ^b (Days)
IC 342	2.1	0.23	43.62	667	759
NGC 253	2.5	1.09	30.78	621	759
M 82	3.3	1.98	17.66	529	705
NGC 4449	3.7	0.08	14.05	483	667
NGC 4945	3.9	1.75	12.64	825	1017
NGC 5128	3.9	0.64	12.64	460	652
NGC 5236	3.9	0.79	12.64	849	1041
CIRCINUS	4.0	1.20	12.02	656	855
NGC 6946	5.5	0.83	6.36	406	763
NGC 5055	7.2	0.53	3.71	0	429

- ^a Distances for each galaxy in the sample are taken from the following authors: (Karachentsev & Tikhonov 1993)(IC 342), (Sreekumar et al. 1993)(NGC 253) (Doane & Mathews 1993)(M82), (Bajaja et al. 1994)(NGC 4449) (Bergman et al. 1992)(NGC 4945, NGC 5128, NGC 5236), (Curran et al. 1998)(Circinus) (Tully 1988)(NGC 6946, NGC 5055)

- ^b Control Time based on a supernova with a [NiII] emission line 3 times brighter than SN11987A

Since the starburst nuclei are dusty, most of the energy produced by stars in the starburst will be absorbed by the dust and re-radiated at far infrared wavelengths. Thus, we can use the far infrared luminosities of the galaxies based on IRAS fluxes to scale the expected supernova rate for each galaxy (e.g. Soifer et al., 1989). This scaling will only be valid if the galaxy nuclei are optically thick in the visible, and if the FIR luminosity measured by IRAS is confined to the region we observe. For starburst galaxies, the starburst nucleus has a radius of a few hundred parsecs (Doane & Mathews 1993). For M82, a 400 pc diameter starburst region extends for 25 arcsec, while our ISO-CAM images extend for 90 arcsec. The galaxy images also show that the infrared emission is strongly concentrated near the nucleus.

From our data, we can derive a confidence level as a function of the supernova rate using Bayesian probabilities (see Sivia, 1996, for an excellent discussion of Bayesian data analysis). Bayes theorem is appropriate for data analysis where we have data and want to derive the probability of a model being true. In this case, the model is simply that supernovae occur randomly with a rate that gives the average time between supernovae and can be detected for a time Δt by observing the [NiII] emission line. The basic equation from Bayes theorem is usually stated as

$$prob(M|D, I) = prob(D|M, I) \times prob(M|I) \quad (5)$$

where M = the model, D = the data, and I = prior information, and all of the $prob()$ are probability density functions. The vertical bar means *given*, so the first term reads *the probability of the model given the data*. As with all probabilities, the total probability is one. The last term is the probability of the model being true given our knowledge of the model and the way our observing process occurs. Since we observe the galaxies at dis-

creet times, t_{obs} , then we will only observe a supernova if it has occurred within a short time, Δt , before the observation. There are then two variables in our model, the supernova rate, which we will call λ , and the time during which a supernova could be detected, Δt . The probability of the data being true, which is that no supernova was seen, is 1 if the observation occurred outside of the observing window and 0 if the observation occurred within Δt of the explosion. If the explosion occurs at t_1 , then

$$prob(M|I) = \begin{cases} 1 & \text{if } t_1 + \Delta t < t_{obs} \\ 0 & \text{if } t_1 < t_{obs} < t_1 + \Delta t \end{cases} \quad (6)$$

We are then left with determining the $prob(D | M, I)$, or $prob(D | \lambda, \Delta t)$, which is the distribution of intervals between events which have a Poisson distribution, and is given by

$$P(\lambda, t) = \lambda e^{-\lambda t} \quad (7)$$

We are really interested in this probability integrated over time, keeping in mind that it is multiplied by $prob(M | I)$. Recalling that the total probability must equal 1, the normalized probability density function of interest is therefore

$$prob(M|D, I) = \Delta t e^{-\lambda \Delta t} \quad (8)$$

We want to place an upper limit on the supernova rate from our data, and so should integrate this probability density function over all rates less than a maximum rate. Integrating over rates from zero to λ_m gives, for a single galaxy, the probability that the rate is less than λ_m of

$$P(\lambda < \lambda_m) = 1 - e^{-\lambda_m \Delta t} \quad (9)$$

For the complete sample of galaxies, we multiply the probabilities of not seeing a supernova in each galaxy when the rate

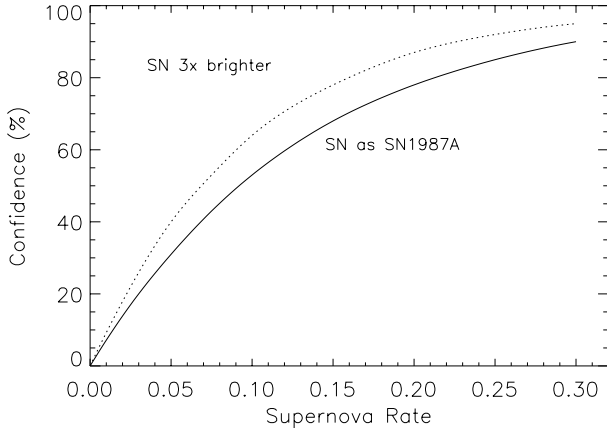


Fig. 6. The confidence (probability) of seeing a supernova in the galaxy sample as a function of the supernova rate in M82. The solid curve is for a supernova with a [NiII] line bright as SN1987A, while the dotted line assumes $3\times$ brighter [NiII] line.

is less than λ_m , then subtract that value from 1 to give the probability of seeing a supernova in our sample. Fig. 6 shows the confidence (or probability) of seeing a supernova as a function of the maximum supernova rate for the entire galaxy sample scaled to M82 for both the SN1987A control time and the $3\times$ SN1987A control time.

The 50% confidence rate, that is the rate which has an equal probability of being correct or incorrect, for supernovae as bright as SN1987A, is 0.09 supernovae per year in M82; the 67% rate is 0.15 supernovae per year, while there is a 90% confidence that the rate is less than 0.30. The derived rates for a supernovae with a [NiII] line $3\times$ brighter than SN1987A, at a confidence level of 50%, 67%, and 90% are 0.065, 0.11, and 0.23 supernovae per year, respectively.

Supernova rates calculated by other authors are usually based on an approach which assumes a constant supernova rate. In that case, the probability of seeing a supernova is just the control time divided by the rate. This approach gives rates at fixed confidence levels which are somewhat less than we calculated using a Bayesian method, resulting in rates of 0.09 (0.065), 0.135 (0.10), and 0.25 (0.19) for confidence levels at 50%, 67%, and 90% respectively; data in parenthesis refers to a supernovae with a [NiII] line $3\times$ brighter than SN1987A.

As a comparison, Van Buren & Greenhouse (1994) derive a rate of 0.1 supernovae per year from radio source counts, assuming that all observed radio sources are supernova remnants, and modeling the evolution of the source brightness with time. They used data from Kronberg et al. (1985), who had derived a rate about twice their value, and quote a result of 0.2 per year from the evolution of radio sources observed by Kronberg & Sramek (1985). Doane & Mathews (1993) and Rieke et al. (1993) considered a supernova rate for M82 of between 0.1-0.3 as fitting the observational data. It is clear from our direct search for recent supernovae that the rate in M82 is highly unlikely to be greater than 0.2 per year. Therefore it is doubtful that there are many supernovae hidden within dusty starburst nuclei or that there is any enhanced star formation in the galaxy cores. In fact

our upper limit for the entire galaxy sample normalized to M82 (0.3 SN per year) translates to a value that is within a factor of 3 of the rate of core collapse SNe (type II + Ib/c) measured by Cappellaro et al. (1999) in a large sample of galaxies; the factor would be even smaller if we compare our results with the rate observed for a sample of IRAS galaxies by Grossman et al. (1999).

4. Summary

We have observed a sample of starburst galaxies at 6.63 μm using ISOCAM to search for the [NiII] emission line characteristic of recent supernovae. While we did not detect any supernovae, we can put upper limits on the supernova rate in M82 of less than 0.3 supernovae per year with a confidence of 90% assuming that the [NiII] line in a supernova will have the same luminosity as the line observed in SN1987A. For a supernova with a [NiII] line 3 times brighter than in SN1987A, the rate is less than 0.23 per year at the 90% confidence level. The corresponding rates for 67% confidence levels are 0.15/0.11 supernovae per year. There is thus no evidence in our data for an enhanced supernovae rate in the nuclei of starburst galaxies.

Acknowledgements. The ISOCAM data presented in this paper was analysed using "CIA", a joint development by the ESA Astrophysics Division and the ISOCAM Consortium. The ISOCAM Consortium is led by the ISOCAM PI, C. Cesarsky Direction des Sciences de la Matière, C.E.A., France.

References

- Antonucci R.R.J., Ulvestad J.S., 1988, ApJ 330, L97
- Bajaja E., Huchtmeier W.K., Klein U., 1994, A&A 285,385
- Bergman P., Aalto S., Black J.H., Rydbeck G., 1992, A&A 265, 403
- Cappellaro E., Evans R., Turatto M., 1999, A&A 351, 459
- Curran S.J., Johansson L.E.B., Rydbeck G., Booth R.S., 1998, A&A 338, 863
- Doane J.S., Mathews W.G., 1993, ApJ 419, 573
- Grossman B., Spillar E., Tripp R., et al., 1999, ApJ 118, 705
- Karachentsev I.D., Tikhonov N., 1993, A&AS 100, 227
- Kronberg P.P., Sramek R.A., 1985, Sci 227, 28
- Kronberg P.P., Biermann P., Schwab F.R., 1985, ApJ 291, 693
- Patat E., Barbon R., Cappellaro E., Turatto M., 1994, A&A 282, 731
- Rank D.M., Pinto P.A., Woosley S.E., et al., 1988, Nat 331, 505
- Richmond M.W., Filippenko A.V., Galisky J., 1998, PASP 110, 553
- Rieke G.H., Loken K., Rieke M.J., Tamblyn P., 1993, ApJ 412, 99
- Sivia A., 1996, A Bayesian Tutorial. Clarendon Press, Oxford
- Soifer B.T., Boehmer G., Neugebauer G., Sanders D.B., 1989, AJ 98, 776
- Sreekumar P., Bertsch D.L., Dingus B.L., et al., 1993, ApJ 426, 105
- Tully R.B., 1988, Nearby Galaxies Catalog. Cambridge University Press
- Turatto M., Mazzali P.A., Young T.R., et al., 1998, ApJ 498, L129
- Van Buren D., Greenhouse M.A., 1994, ApJ 431, 640
- Van Buren D., Norman C.A., 1989, ApJ 336, L67
- Wooden D.H., Rank D.M., Bregman J.D., et al., 1993, ApJS 88, 477
- Woosley S.E., 1988, ApJ 330, 218
- Woosley S.E., Weaver T.A., 1995, ApJS 101, 181